

CFD ANALYSIS OF INDOOR CHEMICAL ENVIRONMENT AND INHALED CONTAMINANT BY A HUMAN BODY

Shuzo Murakami¹⁾, Shinsuke Kato¹⁾, Kazuhide Ito²⁾, Tatsuya Hayashi¹⁾

¹⁾ Institute of Industrial Science, University of Tokyo, Tokyo, Japan

²⁾ Tokyo Institute of Polytechnics, Kanagawa, Japan

ABSTRACT

Indoor air quality is greatly affected by the emission and sorption of chemical compounds from building materials such as VOCs (Volatile Organic Compounds). This paper presents physical and mathematical models and CFD (Computational Fluid Dynamics) analysis of VOCs transportation from the micro scale (inside building materials) to the macro scale (within a room). Furthermore, the micro climate around a human body is analyzed from the viewpoint of inhalation of chemical compounds.

In the micro scale analysis within building materials, physical models of diffusion and sorption of VOCs, which is based on the fundamental physicochemical principles, are proposed. Long-term diffusion analyses in building materials are carried out based on the model equation.

In the analysis of experimental chamber scale, the emission and diffusion of chemical compound within a FLEC (Field and Laboratory Emission Cell) is investigated as the case study of CFD analysis, using the proposed physicochemical models. The problems of emission testing methods using a FLEC are clarified through this CFD analysis.

In the analysis of room scale, the performance of the proposed physical models is evaluated quantitatively in a test room using the technique of CFD. The results of the numerical analysis show that the physical models and their numerical simulations effectively explain how VOCs are generated and transported in a room.

Lastly, the inhalation of contaminated air by a human body is analyzed by CFD. New indices for evaluating the contribution ratio of pollutant source to inhaled air are proposed.

1. INTRODUCTION

IAQ (Indoor Air Quality) is one of the most important factors when designing a healthy indoor climate. To be able to inhale clean air is a fundamental right of human beings. Figure 1 shows the composing ratio of weight of various materials which a human body takes in. The contribution of indoor air by breathing is the largest, amounting to 69% (57+12). This value is much larger than the contribution by eating and drinking. We can thus realize the importance of keeping the indoor air clean in daily life.

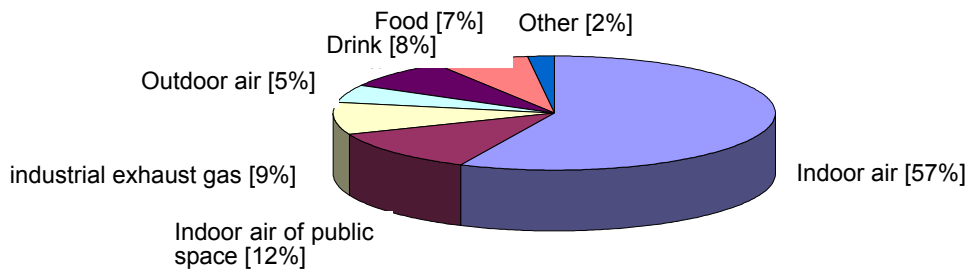


Figure 1 Composing ratio of weight of various materials taken in by a human body

In this study, a method for predicting the distribution of chemical pollutants emitted in a room is investigated. The quality of air inhaled by the human body is also analyzed. Indoor air quality is greatly affected by the emission and sorption of chemical compounds from building materials (Bluyssen, P.M. et al.², Haghghat et al.⁴; Yu, J.-W. et al.¹⁶). In this paper, physical models of emission and sorption of chemical compounds such as VOCs are proposed and examples of CFD analysis are shown.

Many factors, including emission, adsorption/desorption, air change rate, and chemical reactions within both the source material and the room air, affect the concentration of chemical pollutants within a room (Murakami. et al.⁷, Wolkoff. P. et al.¹³.) as shown in Figures 2 and 3. The goal of this study is to predict the concentration of chemical pollutants in the air inhaled by the occupants within a room with such complicated emission/diffusion processes.

2. PHYSICAL AND MATHEMATICAL MODELING OF EMISSION, DIFFUSION AND SORPTION EFFECT

Internal and external diffusion from building material into the room air are modeled as shown in Figure 4. The diffusion and adsorption of VOCs within a porous material is modeled as shown in Figure 5. Furthermore, the modeling of adsorption and desorption of VOCs on the surface of sorptive material is illustrated in Figure 6. Mathematical models for transfer of VOCs are proposed in Table 1, considering the physical processes shown in Figures 4,5,6.

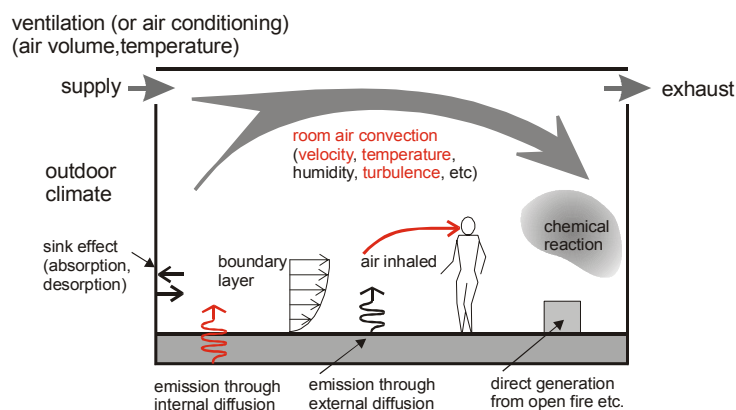


Figure 2 Mechanism of transport and diffusion of VOCs within a room

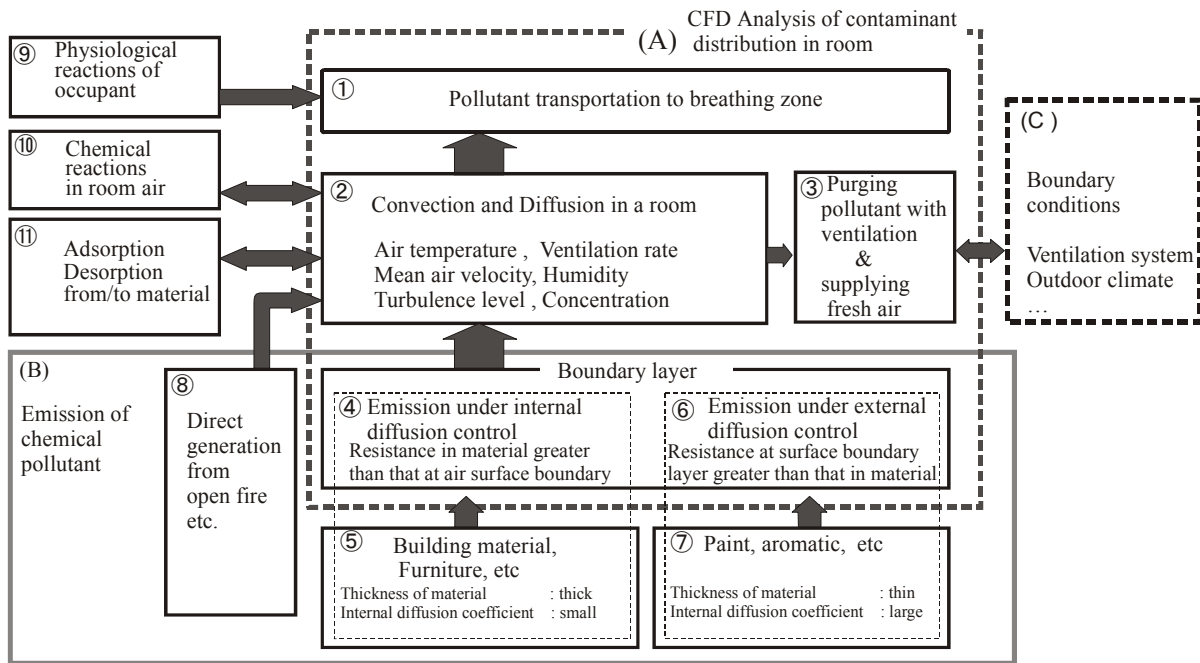


Figure 3 Various factors affecting emission, adsorption and diffusion of VOCs in room

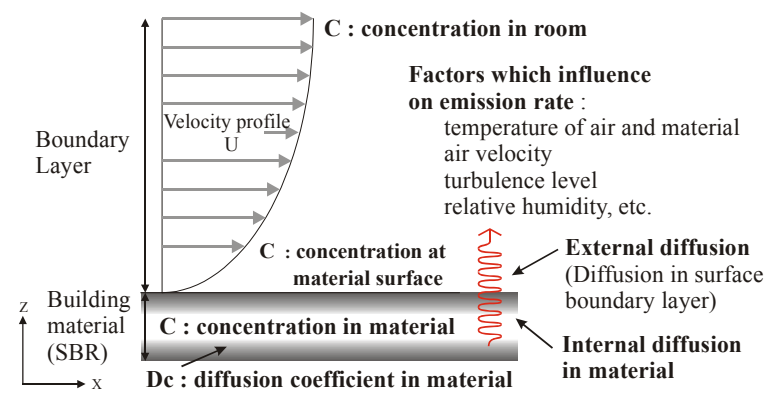


Figure 4 Internal and external diffusion from building material

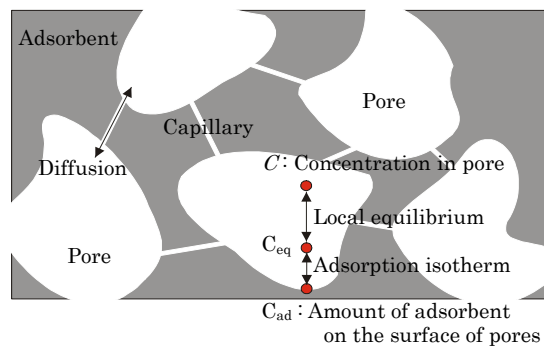


Figure 5 Modeling of diffusion and adsorption of VOCs within porous material

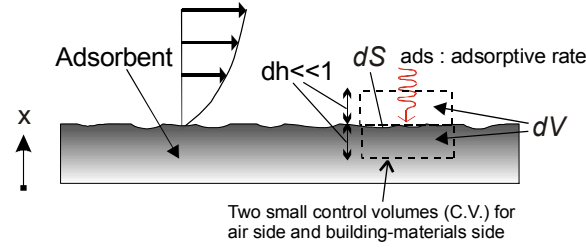


Figure 6 Modeling of adsorption and desorption of VOCs on the surface of sorptive material

Table 1 Physical and mathematical models for VOCs transfer

[1] Transportation of VOCs in room air

$$\rho_{air} \frac{\partial C}{\partial t} + \rho_{air} \frac{\partial(u_j C)}{\partial x_j} = \frac{\partial}{\partial x_j} \left(\left(\lambda_a + \frac{\rho_{air} v_i}{\sigma} \right) \frac{\partial C}{\partial x_j} \right) \quad (1)$$

[2] Conservation of VOCs in porous material with diffusion and adsorption

$$k\rho_{air} \frac{\partial C}{\partial t} = \frac{\partial}{\partial x_j} \left(\lambda_c \frac{\partial C}{\partial x_j} \right) - \rho_{sol} \frac{\partial C_{ad}}{\partial t} \quad (2)$$

[3] Sorption Equilibrium, Local Equilibrium

$$C_{ad} = f(C_{eq}, T) \quad (3)$$

$$C_{eq} = C \quad (4)$$

Eqs. (3) and (4) is necessary for closing Eq. (2).

[4] Diffusion equation for VOCs based on effective diffusion for porous material from Eqs. (2), (3) and (4),

$$\left(k\rho_{air} + \rho_{sol} \frac{\partial f}{\partial C} \right) \frac{\partial C}{\partial t} = \frac{\partial}{\partial x_j} \left(\lambda_c \frac{\partial C}{\partial x_j} \right) - \rho_{sol} \frac{\partial f}{\partial T} \frac{\partial T}{\partial t} \quad (5)$$

when neglecting thermal effect,

$$\rho_{air} \frac{\partial C}{\partial t} = \frac{\partial}{\partial x_j} \left(\rho_{air} D_C \frac{\partial C}{\partial x_j} \right) \quad (6)$$

$$D_C = \lambda_c / \left(k\rho_{air} + \rho_{sol} \frac{\partial f}{\partial C} \right) \quad (7)$$

[5] Boundary condition for flux of C at air-material interface

$$-\rho_{air} D_C \frac{\partial C}{\partial x} \Big|_{B+} = -\lambda_a \frac{\partial C}{\partial x} \Big|_{B-} \quad (8)$$

[6] Simple model for boundary condition at sorptive surface

$$-\lambda_a \frac{\partial C}{\partial x} \Big|_{B-} = -adv \cdot \frac{dV}{dS} = -ads = - \left(\rho_{sol} \frac{\partial C_{ad}}{\partial t} \right) \frac{dV}{dS} = -\rho'_{sol} \frac{\partial C_{ad}}{\partial t} \quad (9)$$

[7] Isotherm models used

[7-1] The Henry model

$$C_{ad} = k_h \cdot C_{eq} \quad (10)$$

from Eqs. (9) and (10),

$$\lambda_a \frac{\partial C}{\partial x} \Big|_{B-} = ads = \rho'_{sol} \frac{\partial C_{ad}}{\partial t} = \rho'_{sol} \frac{\partial k_h \cdot C_{eq}}{\partial t} = \rho'_{sol} k_h \frac{\partial C|_{B-}}{\partial t} \quad (10-1)$$

[7-2] The Langmuir model

$$C_{ad} = \frac{C_{ad0} k_l C_{eq}}{1 + k_l C_{eq}} \quad (11)$$

$$\lambda_a \frac{\partial C}{\partial x} \Big|_{B-} = ads = \rho'_{sol} \frac{\partial C_{ad}}{\partial t} = \frac{\rho'_{sol} C_{ad0} k_l}{(1 + k_l C|_{B-})^2} \cdot \frac{\partial C|_{B-}}{\partial t} \quad (11-1)$$

[7-3] The Polanyi DR model

$$C_{ad} = C_{ad0} \cdot \exp\left(-k_p \left(\frac{T}{V_m}\right)^2 \cdot \ln\left(\frac{C_{sat}}{C}\right)^2\right) \quad (12)$$

$$\lambda_a \frac{\partial C}{\partial x} \Big|_{B-} = ads = 2 \cdot \rho'_{sol} \cdot k_p \cdot (T/V_m)^2 \cdot C_{ad0} / C|_{B-} \cdot \ln\left(\frac{C_{sat}}{C|_{B-}}\right) \cdot \exp\left(-k_p \left(\frac{T}{V_m}\right)^2 \ln\left(\frac{C_{sat}}{C|_{B-}}\right)^2\right) \cdot \frac{\partial C|_{B-}}{\partial t} \quad (12-1)$$

C	: vapor phase concentration in pores and in room-air
C _{ad}	: adsorbed phase concentration on the surface of a pore
ρ _{sol}	: net density of sorptive material
ρ' _{sol}	: plane density of sorptive material
λ _c	: mass conductivity of VOCs in air within a pore
k	: porosity of material
D _c	: effective diffusion coefficient of VOCs in material (effect of adsorption is included)
B+	: air-material surface in material-side region
ads	: adsorption velocity
k _h	: Henry's coefficient
k _l	: Langmuir's coefficient
k _p	: Polanyi's coefficient
C _{sat}	: Saturated concentration,
V _M	: Molecular volume

3. CFD ANALYSIS OF VOCs DISTRIBUTION IN ROOM

The room model shown in Figure 7 is used for analyzing the emission, diffusion of VOCs and the effect of flushing. The room model (2D) has dimensions of (x) × (z) = 75 L₀ × 50 L₀ (= 4.5m × 3.0m; L₀ = 0.06m = width of supply inlet). As the VOCs source, a polypropylene styrene-butadiene rubber (SBR) plate (0.25L₀ thick) was adopted. The emission rate is strongly related to both the initial concentration distribution (C₀(z)) and the effective diffusion coefficient (D_c) within the SBR. Thus, it is very important to evaluate accurately the set of C₀(z) and D_c in the source material.

In this paper, the initial VOCs concentration distribution in SBR is assumed to be uniform, i.e. C₀ = 1.92 × 10⁸ μg/m³. The effective diffusion coefficient D_c is given as 1.1 × 10⁻¹⁴ m²/s (at 23°C) in accordance with Yang et al¹⁵.

Contaminated room air can be flushed by ventilation at a greater air change rate. In this study, the effect of regular flushing (increase in ventilation rate once a day) is investigated. The daily pattern of this intermittent increase in ventilation rate is called 'flushing' in this paper.

Flowfields were analyzed by CFD with a low Reynolds number k-ε model (MKC model) (Murakami et al⁹) with an inflow velocity of 1/10 U₀ (= 0.1 m/s; air change rate = 1.6 h⁻¹) under ordinary conditions (with no flushing) and U₀ (= 1.0 m/s; air change rate = 16 h⁻¹) during

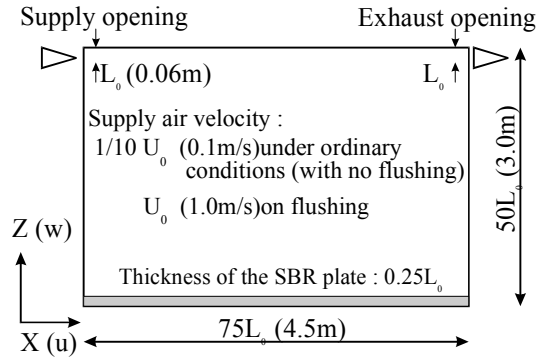


Figure 7 Room model analyzed

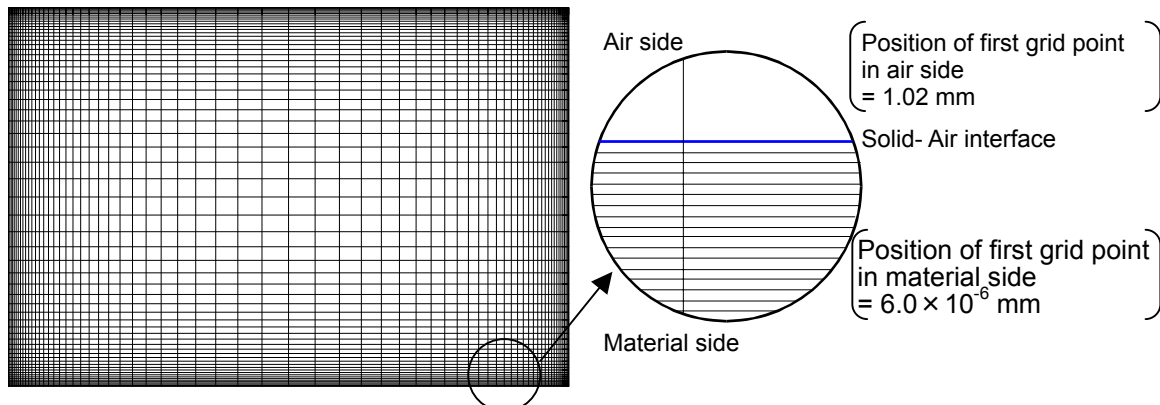


Figure 8 Grid layout within room air and floor plate

Table 2 Cases analyzed

	case1	case2	case3
Hours of air flushing	No flushing	1h/24h	8h/24h
Temperature	23°C		
$D_{eff} : 1.1 \times 10^{-14} \text{ m}^2/\text{s}, Da : 5.9 \times 10^{-6} \text{ m}^2/\text{s}, C_0 : 1.92 \times 10^8 \text{ } \mu\text{g}/\text{m}^3$			

Inflow velocity with no flushing : $U_{in}=1/10 U_0=0.1\text{m/s}$
 Inflow velocity at Flushing : $U_{in}=U_0=1.0\text{m/s}$

flushing. The grid design for CFD analysis is shown in Figure 8. In the computation of CFD, an upwind scheme was used for the convection term, and a centered difference scheme for the diffusion term. Using the results of flow field simulations, emission and diffusion fields were analyzed. In the emission and diffusion analysis, time-dependent Eqs. (1) and (6) were solved by coupling Eq.(8) as the boundary conditions between the solid material and the room air. Table 2 shows the cases analyzed. Three cases were examined in total, under different conditions of inflow velocity (i.e. different air change rate). The time history of room air concentration was obtained over a duration of $2.0 \times 10^7 T_0$ (T_0 ; representative time scale defined by L_0/U_0 , 14 days).

The predicted results of the change of room-averaged concentration after the normalized time of 4.3×10^6 (3 days) are shown in Figure 9. The change of room-averaged VOCs concentration (in case 1) from the 5th day to the 14th day is pretty small over a duration of 10 days in case 1

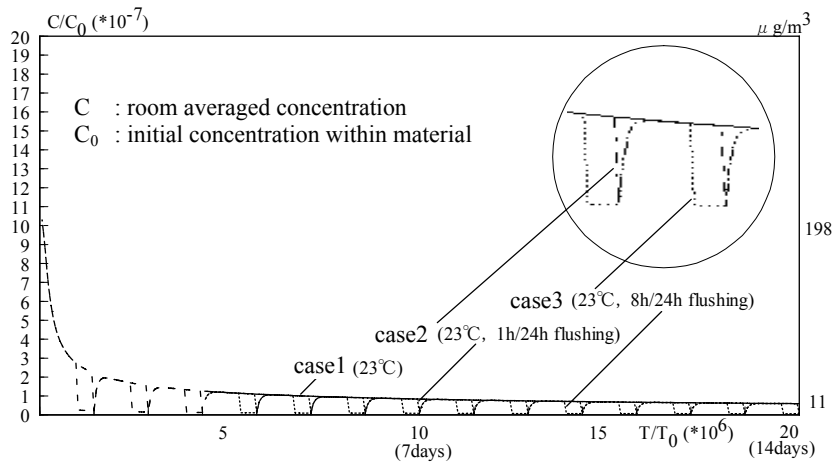


Figure 9 Time history of room-averaged concentrations (C/C_0)

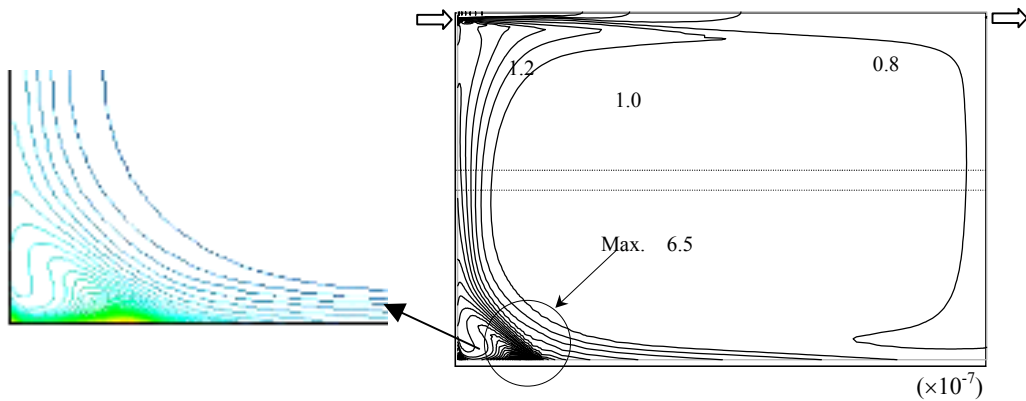


Figure 10 VOCs concentration C/C_0 (at $T/T_0=7.2 \times 10^6$ (5 days, case1))

(no flushing). Case 2 (1-hour flushing per 24 hours) and case 3 (8-hours flushing per 24 hours) show that room-averaged VOCs concentrations decrease to 1/10 of case 1 (no flushing) during the flushing time, as shown in Figure 9.

The concentration distribution within a room is shown in Figure 10. The distribution is not uniform, and is highly non-uniform near the floor.

The averaged concentration of VOCs (C_{ext}/C_0) at the exhaust opening is 0.7×10^{-7} as shown in Figure 10. The room-averaged concentration normalized by the concentration at the exhaust is 1.5 for the condition used here, in which VOCs are emitted from the SBR floor. If the room air were perfectly mixed, the room-averaged concentration would necessarily be the same as that at the exhaust. A value of 1.5 means that the room is not effectively ventilated compared to the case in which the air is perfectly mixed. The VOCs concentration at the left corner near the SBR floor are seven times higher than the room-averaged VOCs concentration. This means that an infant, a child, or a person sleeping on the floor, are highly likely to be exposed to a higher VOCs concentration (as illustrated in Figure 11). The averaged VOCs concentration in the breathing zone with standing posture (C_{ave}/C_0 , $z=25L_0$) is about 1.1×10^{-8} , whereas that with lying posture is about 8.0×10^{-8} .

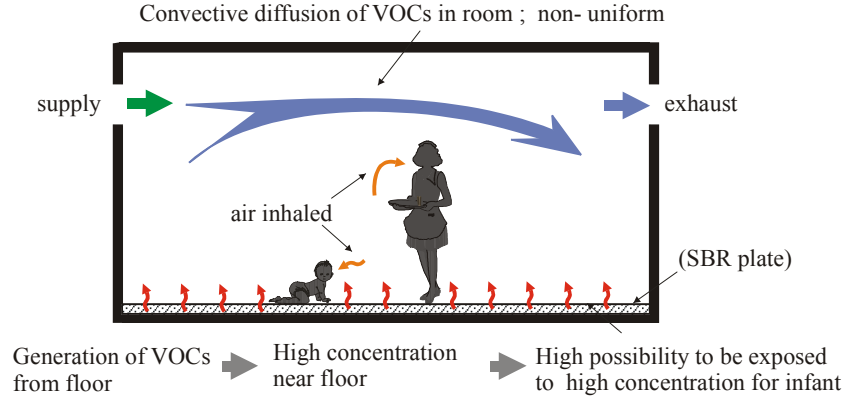


Figure 11 Non- uniform concentration of VOCs in room

4. Prediction of Long-Term VOCs Emission by Analytical Method

4.1 One-dimensional diffusion equation and exact solution

The concentration distribution within a building material of plate type is usually expressed by a one-dimensional diffusion equation, as shown by Eq(6) in Table 6. In this case, we can get analytically the exact solution of Eq(6), by assuming an appropriate boundary condition (Kondo et al⁵). As the concentration C_b at the material surface facing to a room air is much much lower than that within the material, C_b can be assumed to be zero. By this assumption, the exact solution of Eq.(6) is given analytically as Eq.(13).

$$C(x, t) = \frac{4C_0}{\pi} \sum_{n=1}^{\infty} \frac{1}{(2n-1)} \exp\left[-D_c \left\{ \frac{(2n-1)\pi}{2L} \right\}^2 t\right] \sin \frac{(2n-1)\pi}{2L} x \quad (13)$$

Consequently the emission flux per unit area is given by Eq.(14).

$$E(t) = -D_c \left. \frac{\partial C}{\partial x} \right|_B = -D_c \frac{\partial C(0, t)}{\partial x} = \frac{2D_c C_0}{L} \sum_{n=1}^{\infty} \exp\left[-D_c \left\{ \frac{(2n-1)\pi}{2L} \right\}^2 t\right] \quad (14)$$

Here ,

- x : position within the material ($x=0$ at the surface of the material and $x=L$ at the back side of the material)
- t : time
- C_0 : initial concentration within the material [kg(voc)/kg(air)], $C_0=C(x,0)$
- D_c : effective diffusion coefficient within the material [m^2/s]
- L : width of the material [m]

4.2 Case studies for evaluating long-term emission

Figure 12 shows the change of the concentration distribution within the material for the time span of 2 weeks to 50 years. These results are given from the exact solution (Eq. (13)). The value of D_c given by X.Yang and Q.Chen¹⁵ etc is used in this analysis. L is set as 1.5 mm here.

The decrease of the concentration within the material for the first year is large. However we can still observe a pretty large value of concentration after 10 years from the start of emission. When the value of D_c is small as used here, a large amount of VOCs is left within the material after 10 years have passed.

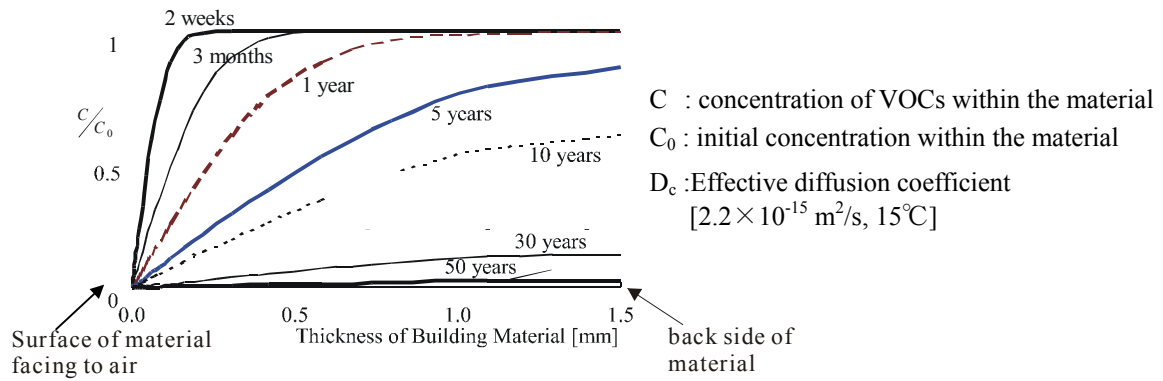


Figure 12 Time history of VOCs distribution within building material

The changes of the concentration of room air for 5 years are shown in Figure 13. This is calculated using the mass balance equation of VOCs emitted, as described in Eq.(15). The emission of VOCs is given by Eq. (14).

$$\frac{dC_r}{dt} = \frac{Q}{V} (C_{in} - C_r) + \frac{M}{V} \quad (15)$$

Here,

- C_r : VOCs concentration in room air
- C_{in} : VOCs concentration of supply inlet
- Q : air change rate
- V : volume of room
- M : emission rate

The concentration of VOCs within the room is assumed to be uniform for each time step. The analysis result for three cases with different values of D_c are illustrated in Figure 13. For the first year, the room concentration with large D_c is higher than that with small D_c , but it is reversed after one year as shown in Fig .13.

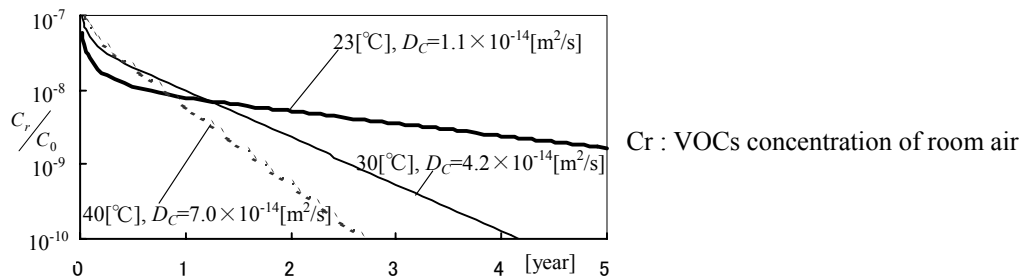


Figure 13 Long term analysis of VOCs concentration in room

5. Application of CFD Technique for analyzing a Diffusion Field within a FLEC cavity.

5.1 FLEC cavity and CFD method

The velocity and diffusion field within the cavity of a FLEC (Field and Laboratory Emission Cell) is investigated using the CFD method, where the chemical compounds (VOCs) are

emitted from the material surface with the cavity. Figure 14 shows the exterior and the section of the FLEC (Wolkoff. P., et al¹⁴). Fresh air is supplied from the thin slot (width of 1mm) at the edge of the cavity. The supplied air is exhausted from the top of the cavity. For the analysis of CFD, the k- ϵ model of a low Reynold's number type (Abe-Nagano model¹¹) is applied. Laminar flow analysis with no turbulence model is also carried out. There were no differences between the velocity fields predicted by both methods of the CFD analysis, i.e. the methods with the k- ϵ model and with no turbulence model. After the flowfield analysis, the diffusion field is computed using the data of the velocity field, by giving the boundary conditions of VOCs emission at the material surface. Here Eqs (1), (6) and (8) in Table 1 are solved by the coupling method.

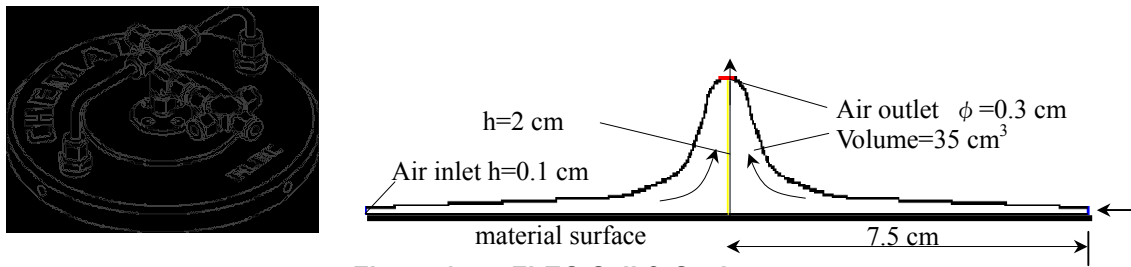


Figure 14 FLEC Cell & Cavity

5.2 Results of prediction for velocity and diffusion fields in FLEC

Three types of emission phenomena from the material are treated here; emission through internal diffusion, emission through external diffusion and the one through mixed material. In the case of internal diffusion, an SBR (styrene-butadiene rubber) plate is used as the emission source. For the analysis of external diffusion, concentration of VOCs is given at the material surface as the boundary conditions. Liquid decane is used for modeling the surface material of external diffusion. For the case of mixed type emission (internal + external), wallpaper + liquid decane is used. In the analysis of internal diffusion and mixed diffusion, the diffusions both within the material and within the cavity air are analyzed. The grid design for the CFD analysis for internal diffusion is shown in Figure 15.

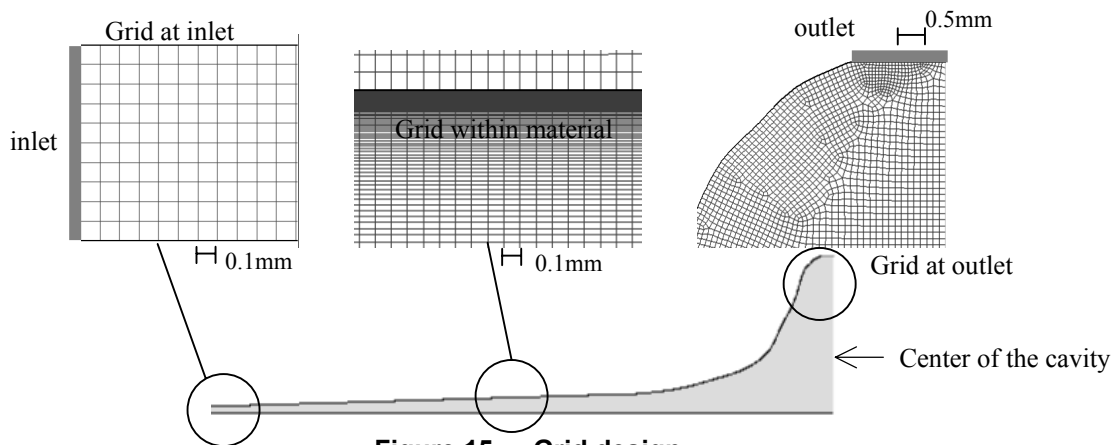


Figure 15 Grid design

The scalar velocity distribution within the cavity is shown in Figure 16. Velocity vector distributions are also shown in Figure 16 for three positions in the cavity. As shown here, velocity values are about 0.5m/s, 2.0m/s except for the exhaust opening. The velocity field is laminar as shown here. Figure 17 shows the velocity distributions near the material surface (at 0.1 mm and 0.5mm from the surface). The velocity near the material surface is bellow 1cm/s.

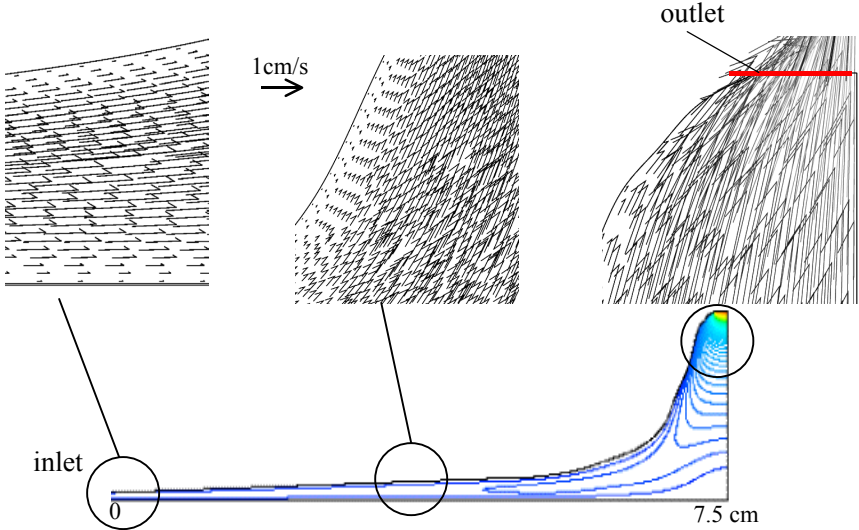


Figure 16 Velocity distribution in FLEC cavity

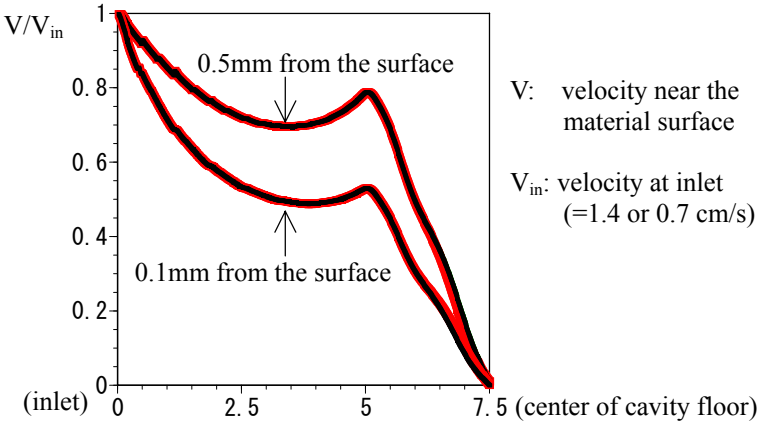


Figure 17 Velocity distributions near the material surface

Figure 18 shows the concentration distribution for the case of external diffusion. Here, liquid decane is used as the surface material for modeling the external diffusion. It is easy to give accurate surface concentration in case of liquid dacane. Hence the emission rate is larger than that of the usual external diffusion material. The emission rate of liquid decane is 6.8(g/m²h) here. The concentration within the cavity increases rapidly just after the inlet and the concentration becomes uniform after this position through the whole space of the cavity. It is required that the VOCs concentration within air should be lower than that at the surface, for measuring the normal diffusion process from the material surface. However it cannot be expected in the case of external diffusion process within a FLEC cavity treated here. Similar

diffusion fields will be reproduced for all types of external diffusion, regardless of the concentration value at the material surface, since the diffusion coefficient D_a in the air is not dependent on the kind of chemical compounds.

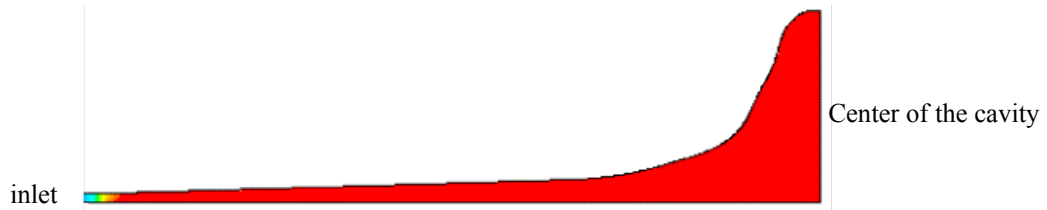


Figure 18 Decane distribution in FLEC cavity (case of external diffusion)

Figure 21 shows the distributions of emission rate (emission flux per unit area) at the material surface for three types of diffusion processes. In the case of external diffusion (Figure 21 (1)), the emission rate is very large at the area near the inlet. However, it becomes zero just after this area. Thus, VOCs are not emitted from most of the area of the material surface within the cavity except for the area just near the inlet, because of the abnormal diffusion field as shown in Figure 18. The emission rate in this situation is likely to be evaluated lower than the correct one.

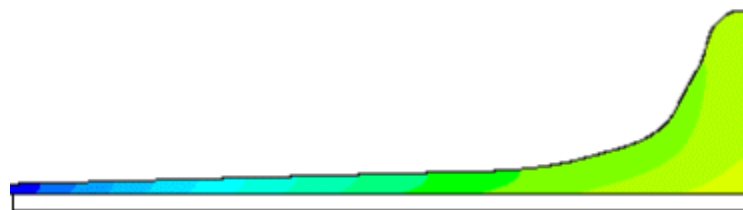


Figure 19 VOCs distribution in a FLEC cavity (case of internal diffusion)

Figure 19 shows the predicted concentration field for the case of internal diffusion. This is the result after 20 hours from the start of measurement with a FLEC. We can observe large concentration gradients both for the horizontal direction and vertical direction. The emission rate from the surface is constant for the horizontal direction, as shown in Figure 21 (2). This result satisfies the condition required for accurate measurement of surface emission. This means that a FLEC performs well for the case of internal diffusion, where the diffusion within the material is also solved.



Figure 20 VOCs distribution in FLEC cavity (case of compound building materials)

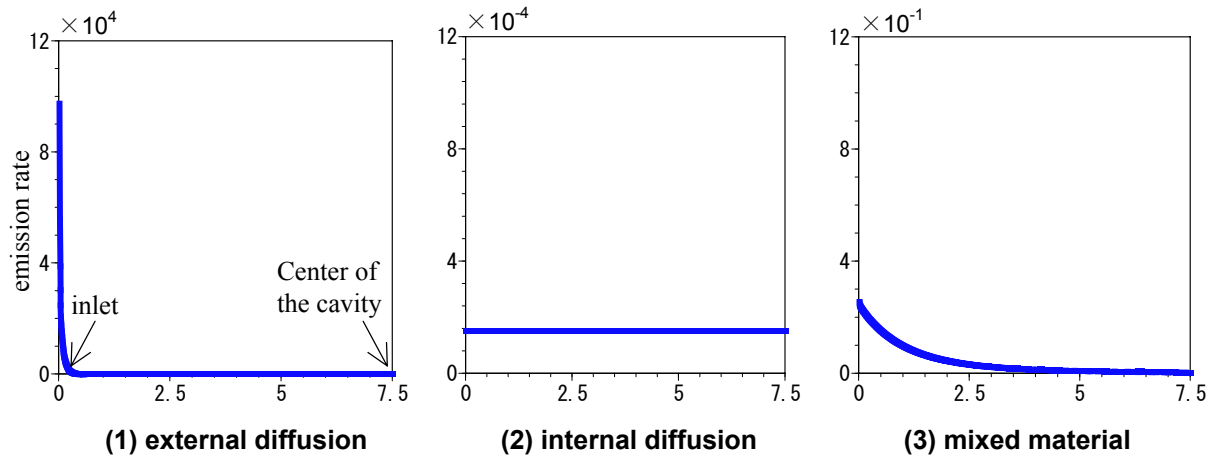


Figure 21 Distribution of emission rate at the surface (emission flux per unit area, $[g/h \cdot m^2]$)

Figure 20 illustrates the predicted concentration field for the case of mixed material (internal + external). The emission rate of liquid decane for the case of mixed material is $6.6 \text{ (g/m}^2\text{h)}$ and is a little smaller than that for the case of simple external diffusion. The thickness of the wallpaper of the mixed material assumed here is pretty thin. Thus, the pattern of the concentration field is similar to the case of simple external diffusion. The emission rate becomes zero at the position behind 30cm from the inlet as shown in Figure 21 (3).

6. CFD Analysis of Quality of Air Inhaled by a Human Body

6.1 Flowfield around a human body

Chemical compounds such as VOCs generated within a room are transported by room air convection and finally exhausted through the outlet opening. In the process of room air convection, some part of the chemical compound is inhaled by the human body. The human body is covered by a rising stream around it, which is generated by the heat discharge due to metabolism. The mechanism of inhalation is affected greatly by this rising stream, as shown in Figures 22 and 25. Figure 22 illustrates the modeling of entrainment of contaminated air near the floor. Figure 25 shows the scalar velocity field around a human body and the velocity vector field around the mouth.

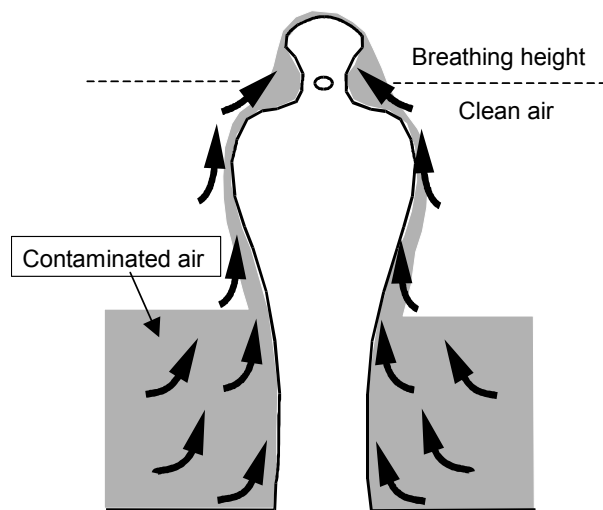


Figure 22 Entrainment of contaminated air near the floor (in the case of calm environment)

6.2 New indices for evaluating contribution ratio of pollution sources

In order to design a healthy indoor climate, we should take into consideration the quality of the air inhaled. Here we propose following new indices for evaluating the relation between the quality of inhaled air and the position of the contaminant source.

1) CRP 1 (Contribution ratio of Pollution source 1)

CRP1 express the ratio of the inhaled amount of the contaminant generated at position i (q_i) to the total amount of the contaminant generated at position i (Q_i). It is defined by Equation 16.

$$CRP1_i = q_i / Q_i \times 100 \quad [\%] \quad (16)$$

q_i : inhaled amount of contaminant generated at position i
 Q_i : total amount of contaminant generated at position i
 i : the position of contaminant source

If the contaminant generated at position i is exhausted to the outside without inhalation by the human body, the value of $CRP1_i$ is 0%. When all contaminant generated at position i is inhaled, the value of $CRP1_i$ is 100%. Figure 23 shows the concept of $CRP1_i$ schematically. When the floor is regarded as one contaminant source, $CRP1_{(floor)}$ is 20% in this example.

2) CRP2 (Contribution ratio of Pollution source 2)

$CRP2_i$ means the ratio of the amount of inhaled contaminant generated at position i (q_i) to the total amount of contaminant inhaled ($\sum q_i$). It is defined by equation 17.

$$CRP2_i = q_i / q_{total} \times 100 \quad [\%] \quad (17)$$

$$q_{total} = \sum_i q_i \quad (q_{total} : \text{total amount of contaminant inhaled})$$

In the example of Figure 23, surface i means various source surfaces in the room. The value of $CRP2$ for the floor is 65% in the example of Figure 23.

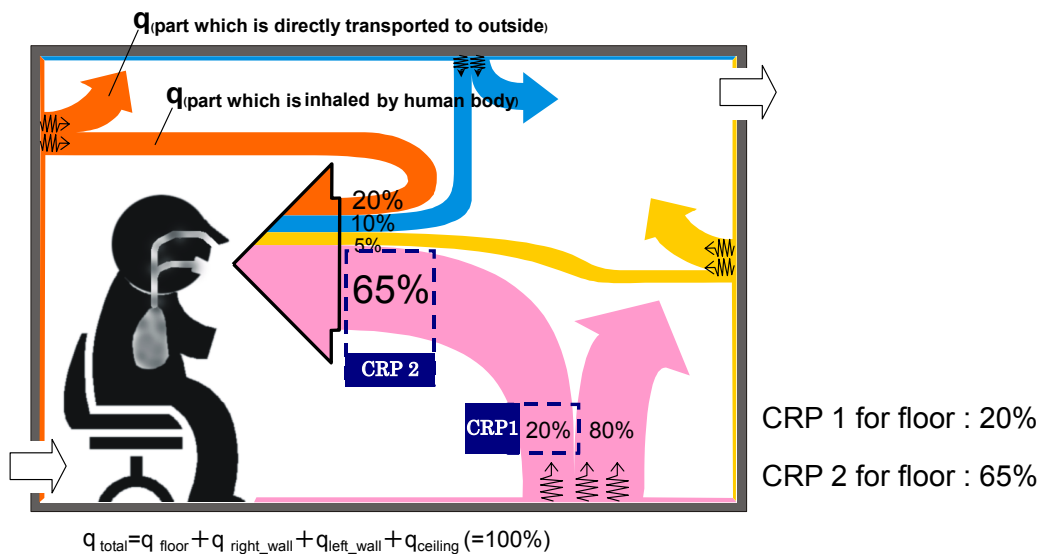


Figure 23 Concept of CRP 1 and CRP 2

6.3 Case studies on CRP1 and CRP2 by means of CFD

6.3.1 Flowfield analyzed

The analysis of CRP1 and CRP2 is carried out using the room model shown in Figure 24. Room air is ventilated with displacement ventilation technique. The flowfield is analyzed by the CFD method with the $k-\epsilon$ turbulence model. The diffusion field is computed using the prediction results of velocity field. Contaminant is regarded as passive scalar.

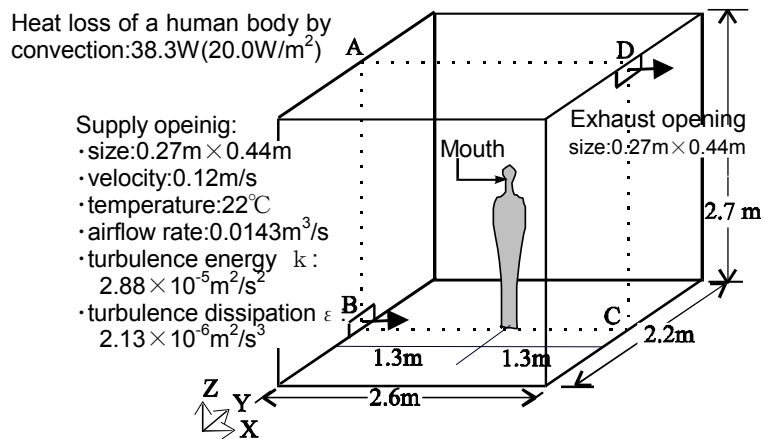


Figure 24 Room model analyzed

Figure 25 shows the predicted flowfield, when a person is standing. A rising stream is well observed around the body as already mentioned. The flowfield with inhalation is visualized by Laser Light Sheet and measured by PIV (Particle Image Velocimeter) as shown in Figure 26. The predicted results of flowfield with inhalation (Figure 25 (2)) corresponds well to the measured value by PIV (Figure 26 (2)).

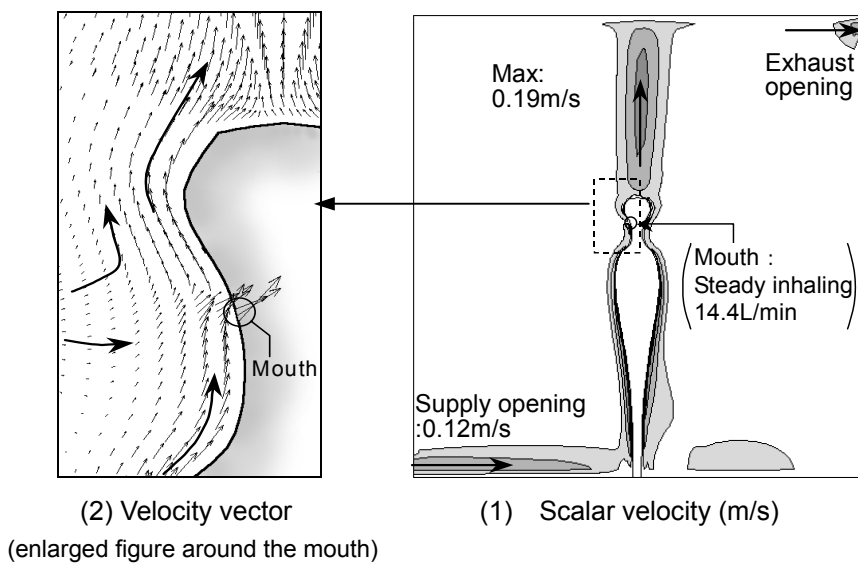


Figure 25 Velocity distributions around a human body

6.3.2 Analysis of CRP1

Predicted results of CRP1 using the data given from CFD analysis are shown in Figure 27. Numbers at each small area of the room surface (i.e. F01~F06 for the floor, W01~W14 for

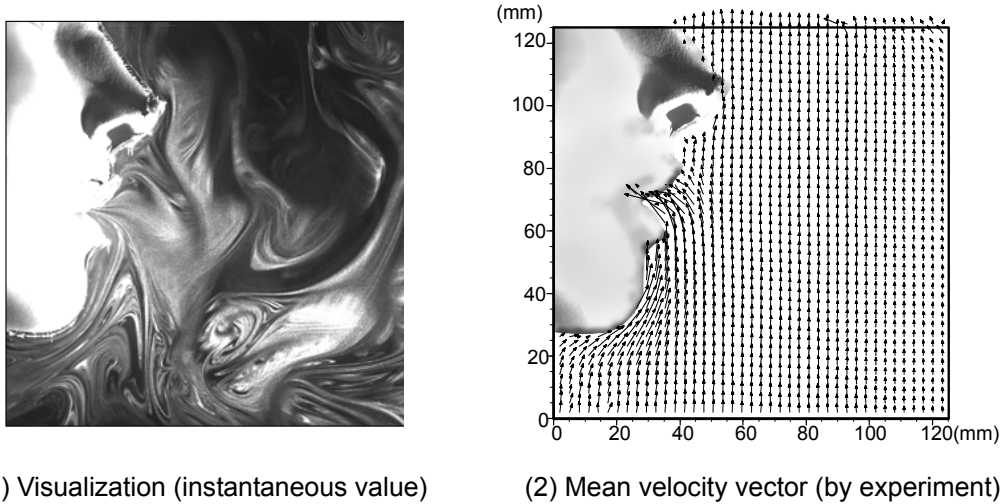


Figure 26 Velocities around mouth of breathing thermal manikin measured with PIV

the walls, C01~C06 for the ceiling) indicate the source position of contaminant (e.g. VOCs). The figures within parentheses at each small area mean the value of CRP1 for each area. The diffusion fields are analyzed for each source position, which corresponds to each small area. Thus, the total number of diffusion analysis is 6+14+6=26. CRP1 is calculated based on each diffusion field. The distribution of the value of CRP1 is separated into two zones, an upper one and a lower one, in this room with displacement ventilation. The values of CRP1 at the lower zone is much larger than those of the upper zone. CRP1 is about 2.6~2.8% for the floor area and 1.66~2.9% for the wall surface area at the lower zone.

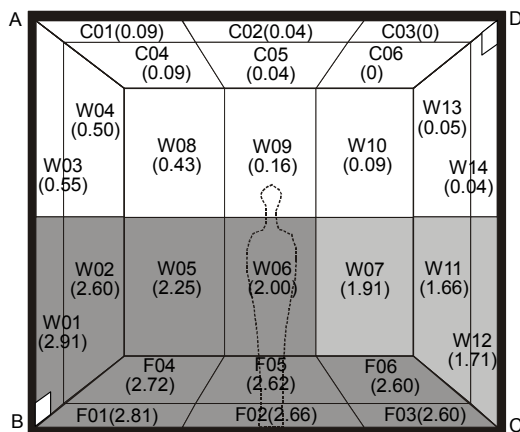


Figure 27 Predicted results of CRP 1

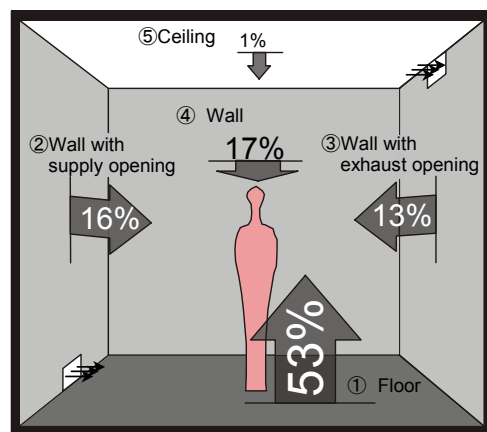


Figure 28 Predicted results of CRP 2

(The value of CRP 1 is shown in the figure in the parentheses)

6.3.3 Analysis of CRP2

The definition of CRP2 is shown in equation 6.2. Suffix *i* means the source position. Here, the source positions are classified as the following 5 ; (1) floor, (2) wall surface with supply opening, (3) wall surface with exhaust opening, (4) other walls, (5) ceiling. It is assumed that the contaminant is generated uniformly at these surfaces. CRP2 of the floor is 52%. This means that over 50% of the inhaled contaminants are occupied by the contaminants generated at the floor. Thus, the reduction of the generation of contaminants at the floor is very effective for decreasing the amount of inhaled contaminant. The values of CRP2 for side walls ((2)~(4)) are about 13~17%. These values are much lower than that of the floor. The contributions of the walls and the ceiling to the inhaled contaminant are pretty small.

CONCLUDING REMARKS

- (1) New physical and mathematical models for analyzing VOCs emission, diffusion and adsorption/desorption processes are proposed. They are well utilized for CFD analysis.
- (2) VOCs transportation from micro scale (within a material) to macro scale (within a room) are analyzed by CFD.
- (3) The concentration of VOCs near the SBR floor, from which the VOCs are emitted, is about seven times larger than that of the room-averaged value.
- (4) New indices for evaluating the inhaled air pollution are proposed. These indices can be utilized with the aid of CFD. They are applied for analyzing the effect of each source position of room surfaces on the inhaled contaminant. The contribution of the floor to the inhaled contaminant is very high.

ACKNOWLEDGEMENT

This study was supported by the Special Coordination Fund for Promoting Science and Technology of the Science and Technology Agency, Japan (Indoor air chemical pollution research for a healthy living environment, chairperson: Shuzo Murakami). Professor Y. Kondo gave us valuable suggestions on this research. The authors deeply appreciate his kind suggestions.

REFERENCES

1. Axley, J.W. 1995. New mass transport elements and compounds for the NIST IAQ model. NIST GCR pp. 95-676
2. Bluysen, P. M., et al., 1995. European database of indoor air pollution sources: the effect of temperature on the chemical and sensory emissions of indoor materials. TNO-Report 95-BBI-R0826.
3. Fanger, P.P., et al. 1988. Air pollution source in offices and assembly halls, Energy and

Building, 12, 93-100

4. Haghighat, F. and de Bellis, L. 1998. Material Emission Rates : Literature Review, and the Impact of Indoor Air Temperature and Relative Humidity. *Building and Environment*, **33**, pp. 261- 277
5. Kondo, Y., Murakami, S., Kato, S., et al., 2000. Modeling of mass diffusion in porous solid and prediction of indoor VOCs concentration based on macroscopic model, Physical model and numerical analysis od VOCs emission from building materials Part 1. *J. Archit. Plann. Environ. Eng., AIJ*, No. 535, 15-21
6. Meininghaus., R, Knudsen., H. N and Gunnarsen., L. 1998. Diffusion and sorption of volatile organic compounds in indoor surface materials, EPIC'98, Lyon, France, 19 - 21 November, vol 1, pp. 33 - 38
7. Murakami, S. et al., 1999. Coupled analysis of emission, sorption and diffusion of chemical pollutants in a ventilated room by CFD, *Indoor Air '99*, Edinburgh, England.
8. Murakami, S., Kato, S., Ito, K. 1998. Coupled Analysis of VOCS Emission and Diffusion in a Ventilated Room by CFD : EPIC'98, Lyon, France, 19- 21 November, vol 1,pp. 19 - 26
9. Murakami, S. et al., 1996. New low Reynolds-number $k-\epsilon$ model including damping effect due to buoyancy in a stratified flow field. *Int. J. Heat Mass Transfer*, **39**, 3483-3496
10. Sparks, L.E., Tichenor, B.A., Chang, J. and Guo, Z. 1996. Gas-phase mass transfer model for predicting volatile organic compound (VOC) emission rates from indoor pollutant sources., *Indoor Air* **6**, pp. 31-40
11. Nagano. Y., et al. 1994. A new turbulence model for predicting fluid flow and heat transfer in separating and reattaching flows- 1. Flow field calculations, *Int. J. Heat Mass Transfer*, Vol. 38. No.1., 139-151
12. Tanabe. S., et al. 1999. Measurement of Aldehydes and VOCs emission rates in two newly constructed houses, *Proc. Of Indoor Air '99*, Edinburgh, Vol.5, 117-122
13. Wolkoff., P. and Nielsen., P. 1996. A new approach for indoor climate labeling of building materials-emission testing, modeling, and comfort evaluation, *Atmospheric environment* Vol. 30. No. 15. pp. 2679 – 2689
14. Wolkoff. P., et al. 1993. Documentation of Field and Laboratory Emission Cell 'FLEC' – Identification of emission processes from carpet, linoleum, paint, and sealant, *Indoor Air*, 3, 291-297
15. Yang, X., Chen, Q., and Bluysen, P. M. 1998. Prediction of short-term and long-term volatile organic compound emissions from SBR bitumen-backed carpet at different temperatures. *ASHRAE*
16. Yu, J.-W. 1987. Adsorption of trace organic contamination in air. Stockholm: Royal Institute of Technology.